

Journal Pre-proof

Groundwater-surface water interactions in a semi-arid irrigated agricultural valley: A hydrometric and tracer-aided approach

Ana Laura Liberoff, María Poca



PII: S0048-9697(23)05250-6

DOI: <https://doi.org/10.1016/j.scitotenv.2023.166625>

Reference: STOTEN 166625

To appear in: *Science of the Total Environment*

Received date: 13 June 2023

Revised date: 16 August 2023

Accepted date: 25 August 2023

Please cite this article as: A.L. Liberoff and M. Poca, Groundwater-surface water interactions in a semi-arid irrigated agricultural valley: A hydrometric and tracer-aided approach, *Science of the Total Environment* (2023), <https://doi.org/10.1016/j.scitotenv.2023.166625>

This is a PDF file of an article that has undergone enhancements after acceptance, such as the addition of a cover page and metadata, and formatting for readability, but it is not yet the definitive version of record. This version will undergo additional copyediting, typesetting and review before it is published in its final form, but we are providing this version to give early visibility of the article. Please note that, during the production process, errors may be discovered which could affect the content, and all legal disclaimers that apply to the journal pertain.

© 2023 Published by Elsevier B.V.

Groundwater-surface water interactions in a semi-arid irrigated agricultural valley: a hydrometric and tracer-aided approach

Ana Laura Liberoff¹, María Poca²

¹ Instituto Patagónico para el Estudio de los Ecosistemas Continentales (IPEEC-CONICET), Boulevard Brown 2915, (U9120ACV) Puerto Madryn, Chubut, Argentina. Corresponding autor. Email: liberoff@cenpat-conicet.gob.ar

² Instituto de Matemática Aplicada San Luis - IMASL, CONICET-UNSL, Av. Italia 1556 (5700). San Luis, Argentina. Email: pocamaria@gmail.com

Abstract

The purpose of this study was to assess hydrological controls (e.g., rainfall, irrigation practices, river discharge, dam operation, evaporation) on surface (SW)- ground water (GW) interactions in an irrigated valley within semi-arid Patagonia, Argentina (-65.49 W, -43.29 S). We combined different sampling designs (watershed/sub-watershed scales, longitudinal and monthly samplings) from 2015 to 2019 to investigate the temporal and spatial variation of hydrometrics, electrical conductivity (EC) and stable isotope composition of surface and ground water. Results showed that plant transpiration in the upper basin, evaporation in the middle basin and the reservoir dynamics modified water salinity and left an imprint in stable isotopes. Water tables in the irrigated valley were high (0.5 – 2 m level from soil surface) and presented higher salinity than river water. Groundwater salinity, temporal variation of water table levels and stable isotopes suggested that groundwater is subjected to evaporation, is recharged from field seepage and, at a lesser extent, from local rainwater. River salinity increased downstream of the irrigated valley during the whole study period (3 years), showing the effects of agriculture and urbanization. EC also responded to the opening and closing of irrigation channels. EC and daily discharge statistical analysis revealed that groundwater recharge the

stream below a threshold discharge of $26 \text{ m}^3\text{s}^{-1}$; with river salinity increasing linearly as daily discharge decrease. This study illustrates the deep modifications that agricultural systems, mainly surface irrigation, produce on semiarid watersheds. Given that SW and GW components are currently not isolated and flow regulation and irrigation practices are playing a critical role in soil quality and river chemistry at low flow conditions, a conjunctive water management strategy must be implemented in order to prevent further land and water quality degradation.

Keywords: environmental tracers, hydrological dynamics, Patagonia water quality

1. Introduction

In many arid and semiarid areas crop production is possible after flow control by dam regulation and provision of irrigation water. Among different types of infrastructure for crop and pasture irrigation, gravity-fed surface irrigation systems remain the most common due to their low cost and low energy requirements (Masseroni *et al.*, 2017). In these systems, water is diverted from surface sources (rivers, lakes, reservoirs) and distributed through a network of canals of different sizes to individual farms, with gravity being the main driving force. Associated with the redistribution of surface water, arid/semi-arid territories are profoundly modified.

In most alluvial valleys, flow regulation and irrigation practices have caused elevation of the water table, soil salinization and land degradation (Benyamini *et al.*, 2005; Scanlon *et al.*, 2007), as well as damage to urban infrastructure and crop yield reduction (Deng and Bailey, 2020). Increased connectivity between surface and ground water, combined with agricultural and farming practices (e.g., application of fertilizers and pesticides) has also resulted in water quality problems in receiving water bodies (Estévez *et al.*, 2018; Pulido-Bosch *et al.*, 2018). However, benefits of groundwater recharge in irrigated semi-arid valleys have been also reported. For example, during the non-irrigation season, groundwater can discharge back to the river and contribute to the base flow during fall and winter (Kendy and Bredehoeft, 2006; Fernald *et al.*, 2010) and under certain scenarios, groundwater recharge can dilute contaminants (Fernald and Guldán, 2006).

To better understand hydrological processes and controls over surface and ground water hydrochemistry a combination of tools and geochemical tracers have been successfully used. Stable isotopic composition of hydrogen ($^2\text{H}/^1\text{H}$, $\delta^2\text{H}$) and oxygen ($^{18}\text{O}/^{16}\text{O}$, $\delta^{18}\text{O}$) provide information about the origin, transport and phase change processes to which the water molecule has been exposed (Gat, 1996). These tracers have been applied to understand hydrological processes by identifying water sources and losses along catchments, as well as prevailing pathways (e.g., Yang and Han, 2020; Letshele *et al.*, 2023). In arid/semi-arid regions, where evaporation and mobilization of soil-stored salts, and therefore soil and water salinization, are important processes (Benyamini *et al.*, 2005; Estévez *et al.*, 2018), measurements of salinity serve as powerful tracers of hydrological processes. When combined with hydrometric approaches that allow the description of flow and water table levels changes in response to rainfall, water pumping, injection and irrigation (e.g., Lamontagne *et al.*, 2005), these tracers provide a promising set of tools for initiating the evaluation of such processes and controls.

The Chubut valley, located in a semi-arid climate in eastern Patagonia Argentina, has 225 km² of irrigated lands. Agricultural and livestock activities rely on surface water from the Chubut River and depend on hundreds of kilometers of irrigation canals of various sizes that transport water to individual farms (Díaz *et al.*, 2021). Water not used by crops or animals returns to the river by surface runoff, through outflow of irrigation and drainage channels. Water intake facilities for the main urban centers in the watershed are located downstream of the agricultural valley and therefore, water quality is subjected to agricultural and livestock practices (Liberoff *et al.*, 2019). As the Chubut River is the most important source of freshwater, human population is highly vulnerable to the impacts of climate change and climate variability (Pessacq *et al.*, 2020; Pessacq *et al.*, 2022).

Surface and ground water are two interacting components of the hydrological system that must be addressed together in order to prevent the loss of ecological functioning and further land and water degradation. Understanding the driving forces behind water fluxes and the spatio-temporal variation

in hydrochemistry is essential knowledge for ecosystem-based management of water resources. In this system, although soil salinization and degradation and water salinity are recognized problems in society, there are only a few research studies published in local journal articles or technical reports that have covered these issues (Laya, 1981; Hernández *et al.*, 1983; Stampone, 2003, 2012, but see Liberoff *et al.*, 2019; Torres *et al.*, 2021). In this study, we evaluated hydrometric and salinity variation of the Chubut River and groundwater within the irrigated valley; we further used stable isotopes as natural tracers of water processes in order to understand interactions between ground and surface water components. The purpose of this study was to assess controls (rainfall, irrigation practices, river discharge, dam operation) on groundwater and surface water hydrochemical dynamics. These findings will improve our understanding of the effect of surface irrigation on the river dynamics in an intensively used semi-arid agricultural valley.

2. Methods

2.1 Study Area

This study focuses on the lower Chubut Valley (Chubut Valley hereafter) located in northeastern Patagonia, Argentina (Fig 1). The Chubut Valley has 225 km² of irrigated lands that produce mainly alfalfa, pasture, horticulture and raise livestock. Water is diverted from the main Chubut River at *Boca Toma* site and is distributed by hundreds of kilometers of irrigation channels of varying sizes to individual farms. The most common method of irrigation is flooding. The irrigation season begin with the opening of the irrigation channels in mid-August and ends with their closure at the end of April. During the rest of the year, water flows only through the main channel of the river. During the month of maximum water demand (January), an approximate flow of 31 m³.s⁻¹ is derived to the irrigation system and distributed over the alluvial plain (Sainz-Trápaga, 2018). Irrigation and drainage channels outflow to the stream at different locations, transporting water that was not used for production. Most of the return flow takes place upstream of Gaiman city (unpublished data, Liberoff A.). Groundwater is used to a greater or lesser extent in rural areas for domestic and livestock purposes and in urban areas within the Chubut Valley for domestic irrigation.

Regarding the geology of the area, the oldest rocks (Lower to Middle Jurassic age) correspond to the volcanic complex named Marifil Formation of continental origin, represented by ignimbrites, lavas and rhyolitic porphyries, volcanic agglomerates, breccias and subordinate tuffs (Consejo Federal de Inversiones, 2013). This formation is considered the basement of the area, floor of the Chubut valley. The flood plain directly linked to the Chubut River, is filled with modern Quaternary material. In general, this material is formed by fine gravels, sands of varied granulometry, and fines (silts and clays) (Consejo Federal de Inversiones, 2013).

Regarding the hydrogeology, it has been reported that Quaternary sediments corresponding to the alluvium rest discordantly on the Tertiary cinerites, forming a single geohydrological system with two sub-systems: a regional phreatic one and a semi-confined component lying in the two eastern thirds of the Chubut Valley (Hernández *et al.*, 1983). A confined aquifer is also present within Tertiary sediments. Stampone (2003) proposed that a semi-permeable clay mantle, which ranges from 1.5 to 4 m, separates the phreatic aquifer. Regionally, the flow of the system is oriented west-east, i.e. towards the Atlantic coast (Hernández *et al.*, 1983).

Semiarid climate in this region is characterized by prevailing winds from the west towards the east, scarce precipitation with relatively weak daily events and extreme dryness conditions (Pessacq *et al.*, 2022). Historical data at Trelew station (located within the Chubut Valley at 13 m a.s.l.), show that the average maximum annual temperature is 20.8 °C, and the average minimum annual temperature is 5.9 °C; the average annual total precipitation is 210.4 mm (Pessacq *et al.*, 2022) with events over 30 mm day⁻¹ considered as extreme rainfall events (Pessacq *et al.*, 2022).

The Chubut Valley is located in the lower basin, in the last stretch of the Chubut River before it flows into the Atlantic Ocean (Fig. 1). Average discharge in this area, measured at Gaiman gauge station, is 34.7 m³sec⁻¹ (1993-2019 record). However, surface water originates in the upper basin; 80% of water yield occurs in 7 sub-basins that represent 20% of the surface area of the entire watershed (57,400 km²) (Pessacq *et al.*, 2015). The Chubut River flows for 1000 km from the western extra Andean

region with an average discharge of $46.4 \text{ m}^3 \text{ sec}^{-1}$ measured at Los Altares gauge station (see Figure 1, Pascual *et al.*, 2020). The hydrograph of the Chubut River has two annual peaks, one in spring due to snowmelt and the other in late fall due to rainfall. The middle section crosses the wide Patagonian plateau from west to east (altitudes ranging from 200 to 600 m a.s.l.) without permanent tributaries. The beginning of the lower basin is defined by the Florentino Ameghino dam site which is located 145 km from the estuary and forms a 71 km^2 reservoir lake inaugurated in 1963 for flood control, irrigation, water supply and energy production.

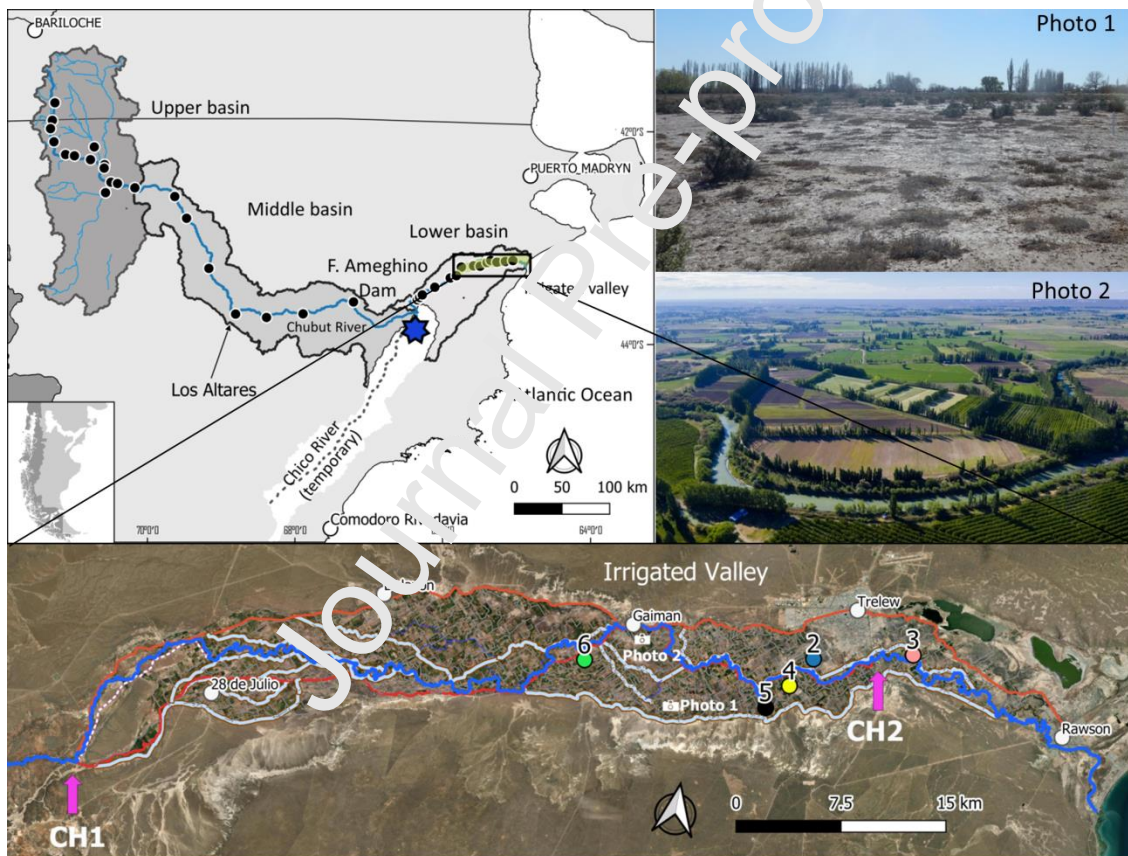


Figure 1. Left-upper panel: location of the Chubut basin in Patagonia, Argentina, and longitudinal surface water sampling. Location of Bariloche and Puerto Madryn stations from Global Network of Isotopes in Precipitation (GNIP) are indicated in white dots. Lower panel: sampling of surface water (arrows) and groundwater (dots) in the Chubut Valley are shown. Main (red) and secondary (light blue) irrigation canals, ditches (gray) and the Chubut river (blue) are also represented. Photo 1 shows

a portion of salinized soil covered by halophytic vegetation (*Suaeda divaricata* Moq., *Atriplex lampa* (Moq.) D. Dietr. and *Salicornia neei*). Photo 2 shows a river reach and surrounding productive lands. The location where the photos were taken are shown on the map (“Photo 1”, “Photo 2”).

2.1.1 April 2017 extraordinary rainfall event

During autumn 2017 an extraordinary rainfall event took place in the region. As described in the results sections, the monthly sampling schedule registered this event and its consequences on water dynamics. It is pertinent to briefly describe this event here in order to interpret the results of this study. Between March 29th and April 8th 2017, an unprecedented rainfall event caused one of the greatest socio-climatic catastrophes of the Chubut Province. The extreme precipitation event reached 399.4 mm, with 232 mm of rain falling on a single day (March 30) in Comodoro Rivadavia city (Fig. 1). Average annual rainfall in this city in the period 1956-2017 is 244.8 mm. Two weeks later the population of the lower Chubut basin suffered the greatest drinking water crisis due to an unusual excess of turbidity in the Chubut River. The environmental cause of this crisis had its origin in the intermittent Chico River basin (Fig. 1). The Chico River only makes flow contributions to the F. Ameghino reservoir during intense storms. During this extraordinary event this tributary carried a maximum flow of 1115 m³/s on April 8th and a volume of 608 Hm³ in three days. As a consequence it contributed an enormous amount of sediment and caused a sudden rise in the level of the F. Ameghino reservoir (11.0 m). The high turbidity in the reservoir and in the Chubut River lasted for almost 60 days, which caused cuts and restrictions to the supply of drinking water for three months.

2.2 Sampling design

In order to evaluate surface (SW) and ground (GW) water interactions in the Chubut valley we analyzed different datasets, compassing two spatial scales. We first explored data from the entire basin (“watershed sampling”) to understand the hydrochemical variation of SW from its source to the mouth (1000 km), the effects of the F. Ameghino dam and to contextualize the lower basin (Fig. 1). To this end, we sampled 35 locations between April 8th and 23rd, 2015, covering the entire

watershed. Then, we examined the hydrochemical data of SW in the Chubut Valley (“Chubut valley SW sampling”) determined at two strategic points along the Chubut River, one upstream of the agricultural valley and the other downstream (Figure 1, lower panel). These measurements were carried out on a monthly basis between August 2016 and March 2019. Discharge data from two gauging stations at the lower basin were used in this study: the Ameghino station located immediately downstream of the dam outlet, and the Gaiman station located in the Chubut Valley (Fig. 1). Daily discharge data for the Ameghino station directly was downloaded from The National Water Information System Data Base¹ (NWI). However for the Gaiman station, we decided not to use discharge data available in the NWI because we detected an overestimation of daily discharge. Upon examining the data, we noticed that the NWI had elaborated yearly H-Q curves with only a few pairs of H-Q measurements each year. We observed that this method overestimated discharge data at the Gaiman station, particularly for the hydrological year 2017-2018. Instead, we elaborated our own H-Q curve using all available H-Q data for the period 1993-2019, using Maximum Likelihood Estimation within the *bbmle* package (Bolker and R development Core Team, 2011) in R software. The estimated flow curve was:

$$Q = 2.66 * H^2 + 10.32 * H - 2.53 \quad (1)$$

Where Q is daily discharge in m³/s and H is water height in m measured at the Gaiman gauge station.

Finally, five pre-existing groundwater wells located in the agricultural valley were also sampled on a monthly basis between August 2016 and March 2019 (“Chubut valley GW sampling”) (Table 1; Fig. 1, lower panel). The water table level was recorded once a month for all wells, except for well 3; the latter had a pumping station and it was not possible to measure the water table level.

Table 1 General information about wells sampled within the agricultural valley

¹ <https://www.argentina.gob.ar/obras-publicas/hidricas/base-de-datos-hidrologica-integrada>

Well No	Sampling method	Usage	Well depth (m)	Water level (m, mean \pm sd)	Electrical conductivity (ms/cm, mean \pm sd)	Linear distance to the river (m)	Sampling period
2	Bailer	no usage	13.82	1.5 \pm 0.3	5.9 \pm 0.41	943	28/10/2016 - 23/08/2018
3	Electric pump	domestic/urban irrigation	9.50	NA	0.57 \pm 0.04	150	22/09/2016 - 26/03/2019
4	Electric pump	domestic/irrigation/livestock	4.20	1.4 \pm 0.3	0.82 \pm 0.12	940	22/09/2016 - 26/03/2019
5	Bailer	no usage	13.90	0.9 \pm 0.2	11.36 \pm 8.58	970	22/09/2016 - 19/07/2017
6	Bailer	no usage (irrigation from Feb 2019)	6.80	1 \pm 1.2	1.92 \pm 0.49	550	22/09/2016 - 26/03/2019

The Chubut valley SW and GW hydrometric and hydrochemical data were explored together with local rainfall data. Daily and monthly precipitation data from the Gaiman station were extracted from the INTA Information System² (Fig. 1).

In-situ electrical conductivity was determined for all samples (Horiba, Model U-10 for samples taken in April 2015 and YSI Professional Plus multi-probe sensor Yellow Springs Instrument Co., Yellow Springs, OH, USA for samples taken between 2016 - 2019). Water samples were stored in 40 mL HPDE vials and shipped to the Isotope Hydrology Section (IAEA, Vienna, Austria) for $\delta^2\text{H}$ and $\delta^{18}\text{O}$ determinations in water.

Stable isotopic compositions of oxygen and hydrogen ($\delta^{18}\text{O}$ and $\delta^2\text{H}$) in surface water and groundwater samples were measured by laser spectrometry at the IAEA laboratories. Oxygen and hydrogen contents are reported in the usual δ -notation (‰, per mil) relative to the Vienna Standard Mean Ocean Water (V-SMOW), after corrections for between-sample memory and normalization to the VSMOW2-SLAP2 scale by using LIMS for Lasers 2015:

$$\delta \text{‰ values} = [(R \text{ sample} - R \text{ VSMOW}) / R \text{ VSMOW}] * 1000 \quad (1)$$

Typical analytical uncertainty of the reported values is about $\pm 0.10 \text{‰}$ for $\delta^{18}\text{O}$ and $\pm 0.8 \text{‰}$ for $\delta^2\text{H}$.

We further calculated the deuterium excess (d-excess) for each water sample following Dansgaard, 1964:

$$d - \text{excess} = \delta^2\text{H} - 8 * \delta^{18}\text{O}$$

² SIPAS, <http://sipas.inta.gob.ar/>

2.3 Data analysis

To assess SW and GW sources and processes occurring at the watershed and sub watershed scales, we used water stable isotopes, meteoric water lines (MWL), d-excess values, and electrical conductivity. Water stable isotopes ($\delta^{18}\text{O}$ and $\delta^2\text{H}$) are natural tracers for water masses because their stable isotopic composition change only through mixing and known fractionation processes that occur during evaporation and condensation (McCallister and del Giorgio, 2012). The Local MWL (LMWL) is a linear $\delta^2\text{H} - \delta^{18}\text{O}$ relationship based on at least one year of local precipitation measurements. The LMWL reflects changes in climate, precipitation seasonality, and geography through deviations in slope and d-excess (Craig, 1961; McGuire and McDonnell, 2007). In this study, we explored precipitation data from Bariloche and Puerto Madryn from the Global Precipitation Isotope Network (GNIP, IAEA- database, Fig. 1) and elaborated a Regional MWL (RMWL) instead of a LMWL (see Results section). Bariloche station has a 5-year track record (1996-1999 and 2002) and Puerto Madryn station has a 3-year record (1999-2001).

For evaluating river and groundwater deviations from the RWML we applied ANCOVA analysis. For the comparison of the $\delta^2\text{H}-\delta^{18}\text{O}$ relationships among wells, we used a parametric bootstrap (Craig, 1961; McGuire and McDonnell, 2007) with 1,000 replicates to estimate the 95% confidence limits for the slopes and intercepts of each well. Statistical analysis and figures were conducted with R software (R Development Core Team, 2020).

To analyze surface the variation in surface water EC under different hydrological scenarios within the irrigated valley, we employed a threshold regression analysis (Fong *et al.*, 2017) using R software (R Development Core Team, 2020). With this analysis we aimed to evaluate whether there is a critical discharge below which river salinity is more affected. The predictor variable was the daily discharge at the Gaiman station while the predicted variable was the difference in EC between CH2 (downstream of the irrigated valley) and CH1 (upstream of the irrigated valley), hereafter referred to as "EC_{valley}". After data inspection we selected the segmented regression model:

$$\text{Segmented regression: } \begin{cases} Y = A_1x + B_1 + C_1 (x < j) \\ Y = A_2x + B_2 + C_2 (x \geq j) \end{cases}$$

Where Y represents ($EC_{\text{valley}} = EC_{\text{CH}_2} - EC_{\text{CH}_1}$) in $\text{mS}\cdot\text{cm}^{-1}$, x is the daily discharge at the Gaiman station in $\text{m}^3\cdot\text{s}^{-1}$, A_i is the regression slope, B_i is the intercept, C_i represents the model residuals and j represents the breakpoint of segmented regression.

3. Results and discussion

3.1 Watershed hydrochemistry dynamics

The LMWL for Bariloche and Puerto Madryn did not differ from each other (i.e. lines are parallel and have statistically the same intercept; $F_{66} = 499.5$, $p_{\text{effect of station}} > 0.05$, $p_{\text{interacción}} > 0.05$, $R^2_{\text{adj}} = 0.96$) (Fig. 2). However, isotopic values from Bariloche ($\delta^{18}\text{O} = -11.1 \pm 3.0$; $\delta^2\text{H} = -81.4 \pm 21.4$; mean \pm standard deviation) were more depleted in ^2H and ^{18}O than values from Puerto Madryn ($\delta^{18}\text{O} = -7.6 \pm 2.9$, $\delta^2\text{H} = -56.1 \pm 20.8$, mean \pm standard deviation.) ($t_{(41.5)} = 4.57$, $p < 0.001$), which is coherent given Bariloche's station is located at a colder and higher altitude area (McGuire and McDonnell, 2007). In light of these results and for data comparison between SW, GW and precipitation, we decided to use a regional meteoric water line ("RMWL") (Fig. 2).

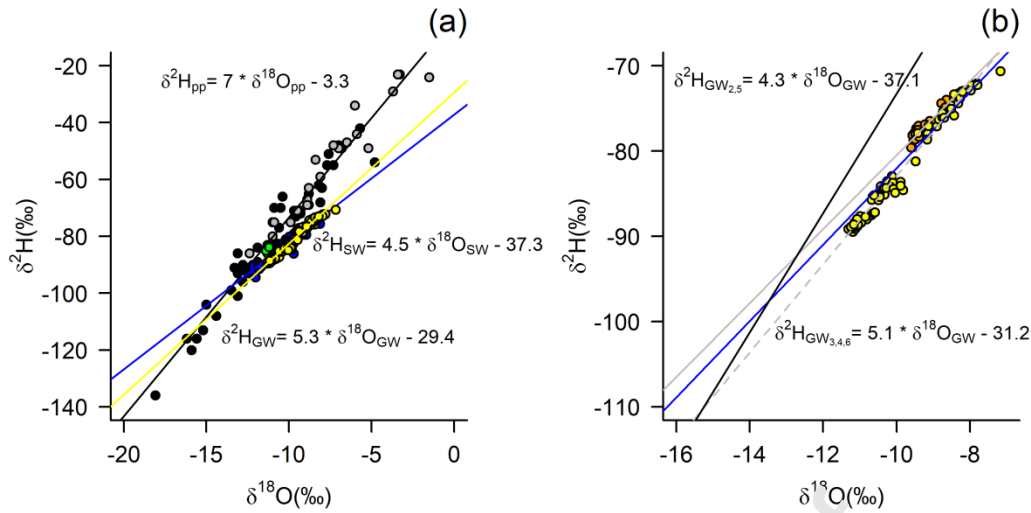


Figure 2. $\delta^{18}\text{O}$ vs $\delta^2\text{H}$ biplot of (a) groundwater (yellow dots), surface water (blue dots) along the Chubut basin and precipitation from Bariloche (black dots) and Puerto Madryn (grey dots). Surface water sampled immediately after the April 2017 event are highlighted as green dots. Regional meteoric water line (RMWL) is shown in solid black, and the evaporation lines of ground (yellow line) and surface waters (blue line) are also shown. (b) Groundwater from shallow wells 3, 4 and 6 (yellow dots and dashed grey line) and deep wells 2 and 5 (orange dots and grey line). RMWL line in solid black and the evaporation line of surface waters (blue line) are also shown.

The isotopic composition of surface water was $\delta^{18}\text{O} = -10.4 \pm 0.8$ and $\delta^2\text{H} = -83.9 \pm 3.8$, while for groundwater was $\delta^{18}\text{O} = -9.5 \pm 1.1$ and $\delta^2\text{H} = -80.6 \pm 5.8$ (mean \pm standard deviation). Water isotopes from the Chubut River samples are located on an evaporation line (McGuire and McDonnell, 2007) that bisects the RMWL at more negative values of $\delta^2\text{H}$ and $\delta^{18}\text{O}$, indicating that the source of the original water is the precipitation at the Andean region (black dots, Figure 2). This is in agreement with the watershed water balance studied by Pessacg *et al.*, 2015, who estimated that more than 80% of water originates in the upper sub-catchments. The $\delta^2\text{H}$ - $\delta^{18}\text{O}$ relationship of GW and SW are located very closely in the biplot (Fig. 2), indicating a close origin and interaction. However, the regression line slopes showed statistically significant differences, with a significant interaction term between factors ($\delta^{18}\text{O}$ and water type –GW vs SW) ($F_{168} = 1661$, $p_{\text{interaction}} < 0.001$, $R^2_{\text{adj}} = 0.953$). The less

steep slope for SW indicates evaporative effects and a steeper slope for GW could indicate that GW is recharging at some extent from rainwater from the lower valley (closeness to precipitation data from Puerto Madryn).

When comparing $\delta^2\text{H}$ - $\delta^{18}\text{O}$ relationships among wells, two groups were found (Fig. 2b). On one hand, wells 3, 4 and 6 showed the same $\delta^2\text{H}$ - $\delta^{18}\text{O}$ relationships (i.e., similar slope and intercept) that differed from those slopes and intercepts of wells 2 and 5. Wells 2 and 5 are the deepest ones and probably reflect deeper phreatic dynamics.

The isotopic composition and EC of surface water determined in April 2015 allowed to distinguish different processes along the watershed (Fig. 3). As the river flowed through the watershed from West to East, EC linearly increased with the distance from the headwater (Fig. 3a). Increasing values of EC were coupled with decreasing values of d-excess only in the middle basin (Fig. 3b). Therefore, salt incorporation in the upper basin might be related to its accumulation due to plant transpiration in the riverbanks (Jobbágy & Jackson 2004), given it is not accompanied by isotopic enrichment and it is assumed that there is no isotopic fractionation during root water uptake (Ehleringer and Dawson, 1992; although, this assumption is being reviewed in the literature). Establishment of exotic plant species, mainly *Salix fragilis*, has expanded significantly on riverbanks of catchments of this region (Datri *et al.*, 2016) shaping the current riparian forest structure in Patagonia (Budde *et al.*, 2011; Thomas *et al.*, 2012). This study provides evidence of transpiration losses which is probably affecting the overall water balance in the upper basin. On the other hand, in the middle basin, salt increase is probably related to evaporation alone, given that EC increases while d-excess decreases.

Below the dam, once the river flows into the valley, there was a steep decrease in EC which might be due to dilution effects in the reservoir and a time-integration effect (i.e., mixing of upstream water from different seasons). This suggests that the evaporative signals observed in both SW and GW in the lower basin (Fig. 1), which originated in the middle basin, become integrated within the reservoir, yielding a distinctive isotope signal. This unique signature helps understanding hydrological processes

and water sources in the lower basin. For instance, surface water sampled during the April 2017 event was located above the RMWL and deviated from the evaporation line for surface water (green dots in Figure 2). This might be reflecting faster runoff in response to the rain event, in contrast to the usual slow runoff that generates the evaporative signals in surface water in the middle basin.

As the river travels through the irrigated valley, there is an evident rise in EC accompanied by relatively minor changes in d -excess values (Fig. 3). As also shown in more detail in the following sections, these changes might be related to the irrigation practices (predominantly flooding) which result in increasing soil salinization. It is worth noting that these results correspond to the beginning of fall that coincides with the end of the irrigation period. The patterns are probably not the same in other moments of the year, such as spring, when the irrigation period begins and most of the snow in the headwaters has already fallen and is melting down and low flows are rising. For specific temporal analysis within the lower valley, please refer to section 3.2.

To summarize, stable isotopes and EC evidence that the Chubut River loses water mainly due to plant transpiration (upper basin) and evaporation (middle basin). Within the reservoir, water originated from snow melting and seasonal rainfall transported through the main stream becomes mixed, and its signals are integrated. This integration yields distinctive stable isotopes signals that allow to understand hydrological processes in the lower basin. SW and GW in the lower valley are closely related and both originate from precipitation in the western region of the watershed.

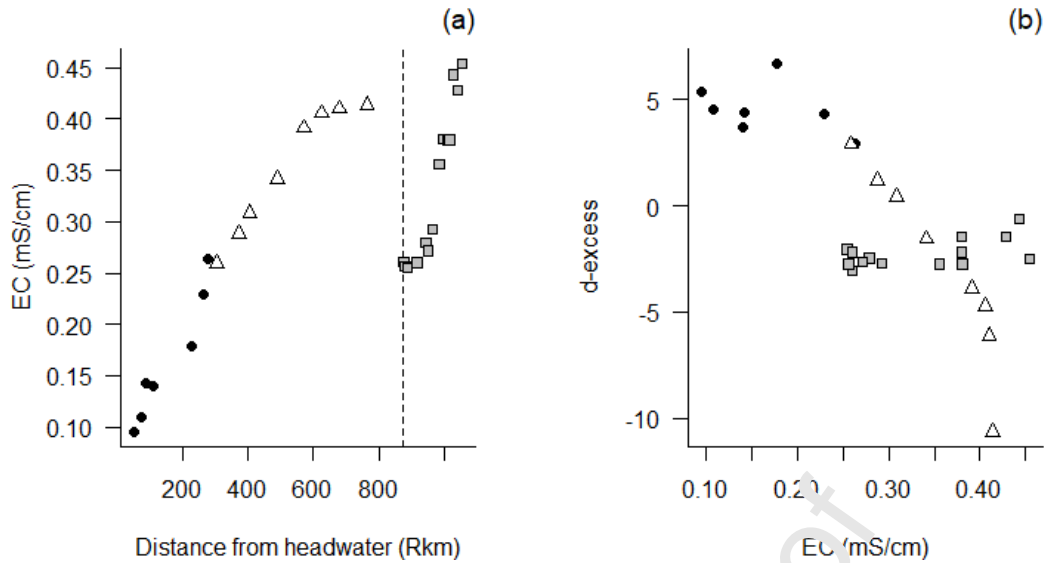


Figure 3. (a) Longitudinal variation of electrical conductivity (EC), vertical dashed line represents the location of F. Ameghino dam (b) d-excess against EC in the upper (filled dots), middle (white triangles) and lower (grey squares) sampled in April 2015.

3.2 Hydrochemistry dynamics in the lower valley

3.2.1 *Surface runoff and rainfall*

During the studied period, 2016, 2018 and 2019 were years with annual cumulative rainfalls (93.6 mm, 93.2 mm and 78.4 mm, respectively) between 37 to 45% below the historical average (210.4 mm) for the lower valley of the Chubut basin. On the other hand, in 2017 the accumulated precipitation reached 263.3 mm, which was 26% above the historical average, which allows us to characterize this one as a wet year. In addition, during 2017 there was a rainfall event above the extreme climatological value that lasted for two days (16 June 2017: 31.3 mm; 17 June 2017: 38 mm) (Fig. 4).

The flow of the Chubut River at the Gaiman station is dependent on the flows delivered by F. Ameghino (Fig. 4). However, there is a significant reduction in daily discharge due to water consumption in the valley, mainly for agricultural purposes (Pascual *et al.*, 2020). The average volume of water used during the irrigation season 2016-2017 was 43 Hm³, 62 Hm³ for 2017-2018 and 28 Hm³

for 2018-2019 (calculated only until March 2019). In response to the April 2017 event and the sudden rise in the F. Ameghino reservoir level (described in Methods Section), a period of highly variable daily discharge and abrupt flow changes, driven by dam operation, was initiated and extended until October 2017. Maximum flows in the order of $84 \text{ m}^3/\text{s}$ were recorded during August and September 2017. On top of April 2017th event, daily streamflow also increased in response to local rainfall events during the months of June 2017 and November 2017 (cumulative monthly rainfall of 97.7 mm and 28.4 mm respectively, Fig. 4). Gaiman flows reached a maximum stormflow of $89.5 \text{ m}^3/\text{s}$ in June 26 in response to the extreme precipitation event that month, which represents a 161.7% surplus to the historical mean monthly flow in June ($34.2 \text{ m}^3/\text{s}$ for the period 1993-2019). Serra *et al.*, 2005 had previously determined that flows in the order of $105 \text{ m}^3/\text{s}$ present critical situations in localized points of the riverbed, therefore this day's discharge almost reached the conveyance capacity of the river channel.

Before and after this particular period, daily streamflow also increased in response to local extreme rainfall events during the months of October 2016, February 2018 and March 2019 (cumulative rainfall of 44.9 mm, 52 mm and 65 mm respectively, Fig. 5). In addition, the discharge at the Gaiman station responded to the opening and closing of irrigations channels. For example, in April 2018, when irrigation channels were closed, discharge increased immediately and it decreased once the channels reopened in August 2018.

In summary, stream discharge in the Chubut valley is mainly regulated by the water delivered by F. Ameghino dam, the volume of water used in the valley, the opening and closing of irrigation channels and at a lesser extent by local precipitation events.

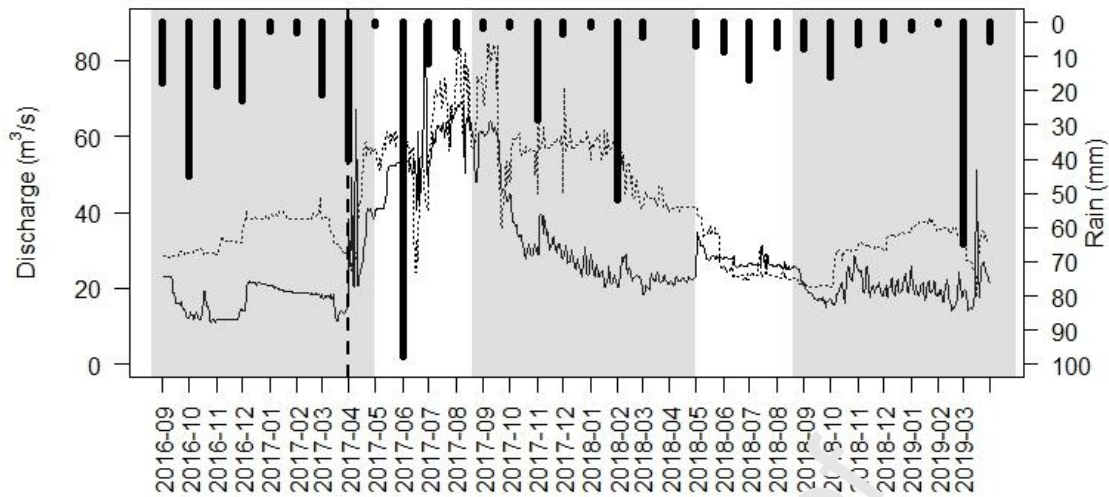


Figure 4. Daily discharge at Ameghino gauge station (dam outlet, dotted line) and Gaiman gauge station (within the irrigation valley, black continuous line) and accumulated monthly rainfall at Gaiman gauge station. Grey bands indicate irrigation seasons.

3.2.2 River salinity

Electrical conductivity values of the Chubut river at site CH2 (downstream the irrigated valley) remained above CH1 values (upstream the irrigated valley) ($EC_{CH1} = 0.29 \pm 0.05$ mS/cm, $EC_{CH2} = 0.41 \pm 0.06$ mS/cm, mean \pm s.d.; $t_{(64.2)} = 8.58$, $p < 0.001$). This increase might be due to a combination of factors such as the application of fertilizers, the mobilization of stored salts in the soil, discharge of irrigation return flows (Estévez et al. 2018 and cites therein) and groundwater recharge (Fernald and Guldan 2006). Urbanization could be also causing an increase in salinity due to discharge of wastewater from cities and industries (Estévez et al. 2018 and cites therein). Although several causes might be mentioned, Chubut River values coincidentally fall within the limit of Spanish rivers with good ecological status (0.40 ± 0.01 mS cm^{-1}) (Estévez et al. 2018).

When evaluating temporal dynamics of EC, discharge and rainfall together, we can identify different hydrological drivers of SW-GW connectivity (Fig. 5). Firstly, the upstream site (CH1) (upstream the irrigated valley) has a relatively stable EC value throughout the studied period. Only the April 2017th

rain event caused an increase in EC that doubled its normal values. This raise in EC can be explained by the extremely high inputs of sediment and water from the Chico basin (Fig. 1) to the reservoir during that event and, consequently, to the lower Chubut River (Kaless et al 2019). This result together with observed EC decline downstream of the reservoir (Fig. 3a) demonstrates the important role of the reservoir in defining downstream salinity.

Below the dam, some EC peaks might be related to local rainfall events, such as the ones occurring in November 2016 and June 2017 (Fig. 5). However, other local rainfall events that led to an increase in daily flow did not result in a corresponding increase in EC (e.g., November 2017, February 2018 and March 2019, Fig. 5). Rainfall and flow pulses play an important role in wetland salinity (Jolly *et al.*, 2008). They cause freshwater pulses that flush stored salts in both the underlying sediments and water column. In addition, increased runoff during rainfall events can increase surface water inflows that are higher in salinity than under natural conditions (Jolly *et al.*, 2008; Letshele *et al.*, 2023). The Chubut River within the irrigated valley is sensitive to local rainfall events in terms of flow, but its behavior related to river EC was variable. The EC peak after the rain event in spring 2016 might be related to low flows that makes the river more sensitive to new inputs of saline water. Conversely, the extreme rainfall event in June 2017 might have caused high runoff from fields and urban centers leading to an increase in river salinity.

Irrigation schedule also affected river salinity. On one hand, the opening of irrigation channels increased EC at the downstream site between August and September 2018. This pattern was not observed in the previous irrigation season (August-September 2017) probably due to the high discharge that flowed as a consequence of the extreme rain events of April and June 2017. On the other hand, after the closure of irrigation channels in 2017 and 2018, a drop in EC was observed at the downstream site. This is probably due to the inflow of more pure and less salty water merely from the dam.

At low flow conditions, as experienced during September 2016 to April 2017, the greatest difference in EC in the river between the upstream (CH1) and downstream (CH2) sites is observed (Fig. 5), indicating a relationship between EC and daily flow. To further analyze this relationship we performed a threshold regression analysis. This procedure was done after removing data that related rises and falls in EC to local or regional rain events (April-2017, Jun-2017) and closure/opening of irrigation channels (May-2018, Aug-2018), as mentioned in the previous paragraphs. The threshold regression analysis indicated a non-linear relationship between EC_{valley} ($EC_{\text{CH2}} - EC_{\text{CH1}}$) and daily discharge (Maximum of Likelihood Ratio Test = 14.83, $p < 0.001$). This analysis also indicated that flow has no effect on EC_{valley} above $26.3 \text{ m}^3 \cdot \text{s}^{-1}$, but EC_{valley} significantly, negatively correlates with daily discharge below this threshold (Fig. 6). The non-linear relationship found earlier indicates that the increase in salinity in the Chubut valley is a consequence of a diffuse dynamic. In addition, data from the watershed sampling, in April 2015, also shows evidence of non-point source of salinity. EC gradually increased throughout the valley (Fig. 3a) when daily flow at Gaiman station ($24.3 \text{ m}^3 \cdot \text{s}^{-1}$, mean daily flow on sampling dates in the Chubut valley; April 18th, 19th and 20th) was below the threshold estimated by the threshold regression analysis. It should be noted that while flow has no effect on EC_{valley} above $26.3 \text{ m}^3/\text{s}$, an increase in salinity is observed from point CH1 to point CH2. This rise may be attributed to other factors mentioned at the beginning of this section (e.g., runoff).

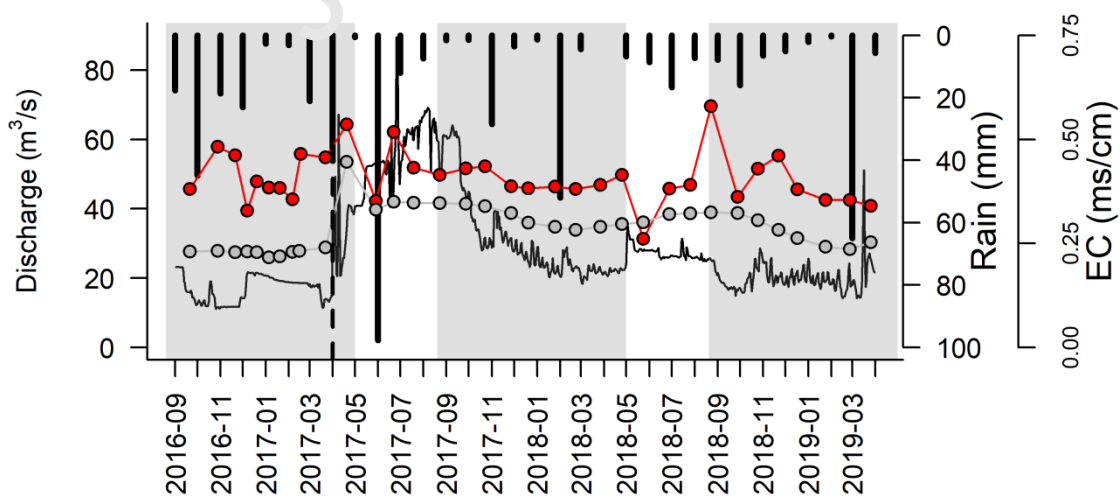


Figure 5. Daily discharge (black continuous line), accumulated monthly rainfall (black bars) at Gaiman gauge station, and electrical conductivity (EC) at two surface water measuring points, upstream (CH1, grey dots) and downstream (CH2, red dots) the irrigated valley. Grey bands indicate irrigation seasons.

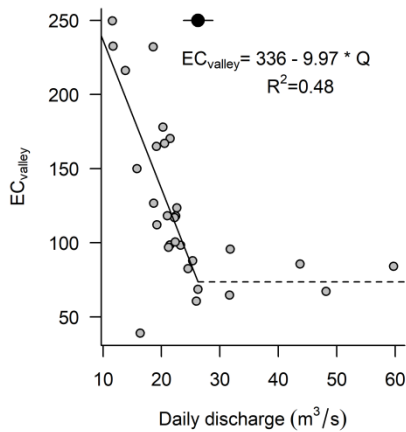


Figure 6. Non-linear relationship between electrical conductivity ($EC_{CH2} - EC_{CH1}$) and daily discharge (Q) at Gaiman station. Solid and dashed lines represent the segmented regression estimated by threshold regression analysis. The dot and whiskers on the top of the plot represent the estimated discharge threshold and its standard error ($26.27 \pm 2.53 \text{ m}^3 \cdot \text{s}^{-1}$).

3.2.3 Groundwater hydrometric and salinity

Over the study period, groundwater levels varied between depths of 0.5 and 2 m (Fig. 7a). The shallowest wells with level records (4 and 6) reached their maximum depths in September 2018, and then, in response to the opening of the irrigation canals the aquifers were recharged. Well 2, one of the deepest ones, showed a similar seasonal pattern that was clearer during 2017-2018 irrigation season, with maximum depths at the beginning and at the end of the season. These patterns indicate a seasonal dynamic of groundwater that is influenced by the irrigation schedule. This seasonal pattern was not observed during 2017. After the April 2017 event, daily flows at the Gaiman gauge station

were above the critical threshold identified in the previous section (Fig. 7a), which might indicate less groundwater recharge to the river and therefore more stable water table levels.

Water table depth is the main factor that influences soil salinization in many alluvial valleys (Benyamini et al 2005). Water table levels reported here are typical of arid/semi-arid alluvial valleys, particularly those with drainage problems and advanced soil salinization problems (e.g., Benyamini et al 2005). Groundwater level seasonal fluctuation, with minimum depths in spring, observed in this system is also typical of irrigated valleys. During spring, irrigation diversions reduce natural stream flows and, at the same time, seepage from irrigation canals and fields (particularly those fields irrigated by flooding) recharges groundwater (Fernald et al 2010, Huang et al 2018).

Groundwater salinity was higher than surface water (Fig. 6, see data above). Groundwater EC varied between wells, with shallower wells 3, 4 and 6 showing lower values than deeper wells 2 and 5 (Table 1). Groundwater EC showed relatively stable values with several temporary peaks during the study period (Fig. 6b). After the April 2017 event was registered for surface water (Fig. 5), all four wells showed a peak in EC and then they rapidly recovered stable values. The high volume of water transported through the irrigated valley as a response of the April event (Fig.4) probably triggered a phreatic climb with mobilization of accumulated salts on the top of the saturated zone. Groundwater of well 6 displayed EC peaks during all summers studied (Jan-Feb-March). However, these peaks might be attributed to different processes. The peak in 2017 is not associated with level variations, rainfall events, or evaporation signals (see following section). In contrast, the peak in February 2018 coincides with a local rain event of 52 mm/month. The peak in 2019 also coincides with a local rain event of 65 mm/month, but the EC rise started prior to the rainfall event. Evaporation of shallow groundwater can occur when the groundwater moves upward into the non-saturated zone (Van Weert et al. 2009). Therefore, EC peak in 2019 might also be related to evaporation during summer given this was the shallowest well (Fig. 7a) and presents evaporation signals (see following section).

Well 2, on the other hand, showed another EC peak that corresponded to a maximum depth (lowest water level) in the seasonal dynamic described in the previous paragraph.

In general terms, increase in salinity of groundwater in relation to river water might result from salt concentration due to plant transpiration and evaporation and/or mobilization of natural high concentration of salts accumulated in the vadose zone, typical from arid/semi-arid regions (Scanlon et al. 2005, 2009) (Fig. 1, see Photo 1 and caption). Water level dynamics and high groundwater EC supports the hypothesis that river salinity dynamics below the discharge threshold found in the previous section respond to the influx of more saline groundwater. High water table levels coupled with low flow conditions in the main stream can create a hydraulic gradient that promotes water fluxes towards the stream (i.e., gaining stream) (Fernald and Guldan 2006). Torres et al (2021) reported that the Chubut River near Gaiman station behaved as a losing stream during winter-spring 2017 whereas at Trelew city groundwater inputs were around 24%. Daily discharge between June and November 2017 (study period in Torres et al. 2021) was never below the threshold identified in this study, however it appears that hydraulic gradients towards the river mouth make the Chubut River a gaining stream. In other irrigated alluvial valleys it has been reported that groundwater discharge sustains streamflow during critical low-flow periods (Kendy 2006, Fernald et al 2010). Return flows in this system can play a significant role in freshwater ecosystem dynamics and surface water base flow maintenance (therefore also providing water for human consumption) given that during winter and fall dam operation is aimed at storing water for months with higher water demands.

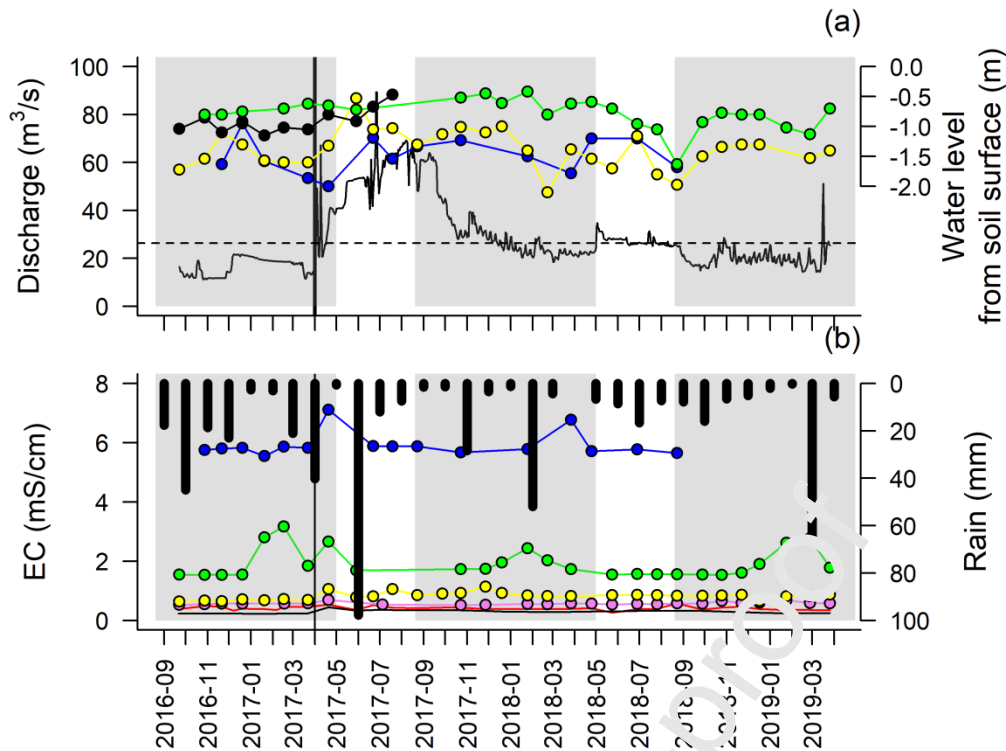


Figure 7. (a) River discharge at Gaiman gauge station (solid black line) and water level from soil surface of wells 2 (blue dots), 4 (yellow dots), 5 (black dots) and 6 (green dots), the dashed line represents the threshold under which flow negatively linearly correlates to EC (section 3.2.2), and (b) Electrical conductivity of surface water at CH1 and CH2 (black and red lines, respectively) and wells 2 (blue dots), 3 (pink dots), 4 (yellow dots) and 6 (green dots). Grey bands indicate irrigation seasons.

3.2.4 Water stable isotopes

Water from both, stream sampling points and wells, exhibited variable temporal dynamics of stable isotopes indicating variation of water sources and times of *in situ* increased evaporation or inflow of evaporated waters (Fig. 8).

Surface water at both sampling points show an increase in evaporative signals (decrease in d-excess values) towards spring 2017 and summer 2018 (Fig. 7a), coinciding with a period of significant flow reduction (Fig. 5). During summer 2019, well 6 shows a decrease in d-excess values which indicate that the increase in EC during this period responded to evaporation.

Prior to the April 2017 extreme rainfall event, wells 4, 5 and 6 had similar $\delta^{18}\text{O}$ values and intermediate d-excess values compared to river water. This is consistent with a high interaction between GW and river water at low flow conditions that might be responsible for the diffuse contribution of salinity evidenced in section 3.2.2. Stable isotopes and d-excess values of surface water clearly recorded the extreme April 2017 event; $\delta^{18}\text{O}$ dropped sharply and d-excess values rose immediately after the event (Fig. 8). However, these changes had no impact on the isotopic and d-excess values of groundwater. Given that this event occurred close to the end of the irrigation season it might be possible that seepage from irrigation canals and fields was not enough to modify stable isotopes signals of groundwater.

When evaluating the entire study period, the difference between the $\delta^{18}\text{O}$ and d-excess values of river water and groundwater decreased over time since the 2017 rain event (Fig. 8). This trend could be associated with the dilution of the regional precipitation signal (originated from the lower Chubut and Chico basins) from the April 2017 event at the reservoir. As time progressed, the river recovered the signal of precipitation from the Cordillera zone. The lasting effect of the April 2017 event was also recorded in dissolved nutrient concentrations (Kaless et al 2019). As a response of this event there was a 6-fold increase in nitrate concentration that slowly decreased and reached stable values in CH1 after Jan 2018 (Kaless et al 2019).

Unlike water level and EC dynamics, stable isotopes allowed to trace the effect of local rainfall. For example, the November 2017 rain event (Fig. 5) seems to have changed the isotope values of river water at CH2 and groundwater measured at well 4 (Fig. 8). During March and April 2018 there is a sudden decline in d-excess at both sampling points that is not coupled with an increase in EC (Fig. 5), as expected if evaporation was the cause of such decline. The change in surface water isotopes could then be related to local rainfall events occurred in February 2018 (Fig. 5) that also caused an increase in salinity in well 6 (Fig. 7). This temporal trend is consistent with results found at the watershed level

that indicated that although the source of ground and surface water is the precipitation at the Andean region, GW is recharging at some extent from rainwater from the lower valley.

After the April 2017 event, well 3 appears to have a stronger coupling with surface water, as it follows the general trend of both the $\delta^{18}\text{O}$ and d-excess curves of the river water over time. This may be explained by the hydraulic connectivity of this well to the watercourse (distance of 150 m, Table 1) and to CH2 surface water measurement point (Fig. 1). Wells 3 and 4 have similar d-excess variation patterns. However, since well 4 is shallower and may be subject to more evaporation (Van Weert et al. 2009), it has, on average, more negative d-excess values. In contrast, well 2 appears to be the least connected to surface water, as it is the most stable in $\delta^{18}\text{O}$, d-excess (Fig. 8) and level values (Fig. 7a), even after the April 2017 extreme event.

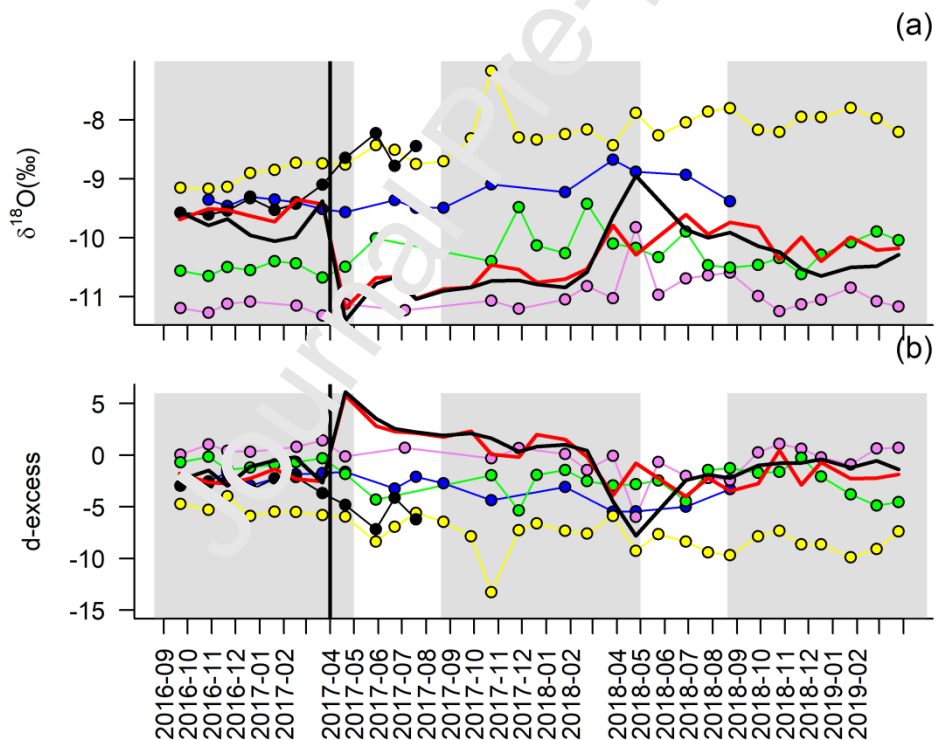


Figure 8. Temporal variation of (a) $\delta^{18}\text{O}$ in surface water upstream and downstream the irrigated valley (CH1 and CH2 represented with black and red lines, respectively) and wells 2 (blue dots), 3 (pink dots), 4 (yellow dots), 5 (black dots) and 6 (green dots), and (b) d-excess of surface and groundwater (symbols are the same as in panel a). Grey bands indicate irrigation seasons.

4. Conclusion: surface and ground water interactions in the irrigated Chubut valley

SW-GW interactions have several impacts on land and water management, wetland ecology, water chemistry and crop production, among others. In this study we identified controlling factors of surface and groundwater hydrometrics and salinity and identified interactions between these both water components in a semi-arid irrigated valley.

Water tracers measured at the lower Chubut valley are influenced by upstream hydrological dynamics. Plant transpiration and evaporation taking place in the upper and middle basin and reservoir dynamics affect water stable isotopes signature and river salinity downstream.

GW and SW in the irrigated valley have a common origin in precipitation from the Andean region, but stable isotopes at the watershed and subwatershed scale evidence that GW is recharging at some extent from rainwater from the lower valley and indicates that shallow groundwater is subjected to evaporation. Groundwater salinity and the temporal variation of water table levels suggest that groundwater is recharged from field seepage. However, since mobilization of salts accumulated in soil and the unsaturated zone is expected, more detailed studies are necessary to differentiate and quantify seepage from irrigation canals to fields.

Stable isotopes temporal trends of GW and SW indicate hydraulic connectivity of shallower aquifers to the watercourse. Results showed that GW-SW interactions are stronger during low flow periods. Regression threshold analysis of surface salinity, water table dynamics, salinity of groundwater and water isotopes in both GW and SW indicate that groundwater recharges the stream below a threshold discharge of $26 \text{ m}^3 \text{ s}^{-1}$ modifying river salinity. Alongside the effect of groundwater recharge, river salinity is largely influenced by agricultural and urban activities, reservoir dynamics, dam operation as well as the opening and closing of irrigation channels. On the other hand, rainfall events increase stream daily flow, but not all rainfall events affect river salinity.

In undisturbed arid watersheds water tables are commonly deep and streams behave as influents, losing water to the aquifer. In these systems, naturally stored salts in the soils are mobilized, diluted and flushed by rainfall events and flooding (Jolly et al 2008). The actual dynamic of the Chubut alluvial valley is the opposite. Flow regulation, artificial groundwater recharge and lack of programs to control water levels are playing a significant role in regulating soil quality and groundwater discharge to the stream under low flow conditions.

Semi-permeable clay layers, like the one reported for this study system (Stampone 2003), can reduce the velocity and quantity of water percolating through the vadose zone and reaching the water table (Ochoa et al 2009). However, it has been also reported that clayey soils form desiccation cracks that actively transports a significant amount of water directly into the deep sections of the vadose zone (Baram et al. 2012). Authors suggested pollutants transported by this preferential flow will bypass the biogeochemically active parts of the vadose zone and compromise groundwater quality. Given that we present evidence of strong GW-SW interactions especially at low flow conditions, pathways of chemicals applied/used in agricultural fields and feedlot facilities must be tracked in order to control and prevent groundwater and surface water quality degradation.

5. Acknowledgments

Funding for this research was provided by the International Atomic Energy Agency (project number F33021), Agencia Nacional de Promoción de la Investigación, el Desarrollo Tecnológico y la Innovación (projects PICT 2015-0138 and PICT 2018-03538) and Consejo Nacional de Investigaciones Científicas y Técnicas to A. Liberoff and was also conducted under the projects “Red para la conservación de los ecosistemas fluviales de la Patagonia” (CONICET) and PUE-IPEEC-CONICET N° 22920160100044. The authors wish to thank Américo Torres for sharing the location of wells, land owners that allowed taking samples and Adrian Contreras and Heriberto Daniel Williams from the Irrigation Company (“La compañía de Riego del VIRCh”). The authors also thank Facundo Irigoyen for his assistance in field campaigns.

6. Bibliography

- Benyamini, Y., Mirlas, V., Marish, S., Gottesman, M., Fizik, E., Agassi, M., 2005. A survey of soil salinity and groundwater level control systems in irrigated fields in the Jezre'el Valley, Israel. *Agric. Water. Manage.* 76, 181-194.
- Bolker, B., R development Core Team, 2011. *bbmle: Tools for general maximum likelihood estimation*. R package version 0.9.7.
- Budde, K.B., Gallo, L., Marchelli, P., Mosner, E., Liepelt, S., Ziegenhagen, B., Leyer, I., 2011. Wide spread invasion without sexual reproduction? A case study on European willows in Patagonia, Argentina. *Biol. Invasions*. 13, 45-54.
- Consejo Federal de Inversiones, 2013. Plan Director de Recursos Hídricos del Río Chubut. Informe Final, tomo I, documento principal.
- Craig, H., 1961. Isotopic Variations in Meteoric Waters. *Science*. 133, 1702.
- Dansgaard, W., 1964. Stable isotopes in precipitation. *Tellus* 16, 436-468.
- Datri, L.A., Faggi, A.M., Gallo, L.A., Carmona, F., 2016. Half a century of changes in the riverine landscape of Limay River: the origin of a riparian neoecosystem in Patagonia (Argentina). *Biol. Invasions*. 18, 1713-1722.
- Deng, C., Bailey, R.T., 2020. Assessing causes and identifying solutions for high groundwater levels in a highly managed irrigated region. *Agric. Water. Manage.* 240.
- Díaz, L., Raguileo, D., Hernández, M., Salvadores, F., 2021. Caracterización del sistema de riego del Valle Inferior del Río Chubut. Análisis desde las representaciones y opiniones de quienes riegan. Centro Regional Patagonia Sur, INTA Ediciones, p. 97.
- Ehleringer, J.R., Dawson, T.E., 1992. Water uptake by plants: perspectives from stable isotope composition. *Plant, Cell & Environment* 15, 1073-1082.
- Estévez, E., Rodríguez-Castillo, T., González-Ferreiras, A.M., Cañedo-Argüelles, M., Barquín, J., 2018. Drivers of spatio-temporal patterns of salinity in Spanish rivers: a nationwide assessment. *Philosophical Transactions of the Royal Society B: Biological Sciences* 374, 20180022.
- Fernald, A.G., Cevik, S.Y., Ochoa, C.G., Tidwell, V.C., King, J.P., Guldan, S.J., 2010. River Hydrograph Retransmission Functions of Irrigated Valley: Surface Water–Groundwater Interactions. *Journal of Irrigation and Drainage Engineering* 136, 829-835.
- Fernald, A.G., Guldan, S.J., 2006. Surface water-groundwater interactions between irrigation ditches, alluvial aquifers, and streams. *Rev. Fish. Sci.* 14, 79-89.
- Fong, Y., Huang, Y., Gilbert, P.B., Formar, S.R., 2017. *chngpt: threshold regression model estimation and inference*. *BMC Bioinformatics* 18, 454.
- Gat, J.R., 1996. Oxygen and hydrogen isotopes in the hydrologic cycle. *Annu. Rev. Earth. Planet. Sci.* 24, 225-262.
- Hernández, M.A., Ruiz de Calarreta, V.A., Fidalgo, F., 1983. Diagnósis geohidrológica aplicada en el valle inferior del Río Chubut. *Ciencia del Suelo* 1, 83-91.
- Jolly, I.D., McEwan, K.L., Holland, K.L., 2008. A review of groundwater–surface water interactions in arid/semi-arid wetlands and the consequences of salinity for wetland ecology. *Ecohydrology* 1, 43-58.
- Kendy, E., Bredehoeft, J.D., 2006. Transient effects of groundwater pumping and surface-water-irrigation returns on streamflow. *Water. Resour. Res.* 42, 1-11.
- Lamontagne, S., Leaney, F.W., Herczeg, A.L., 2005. Groundwater-surface water interactions in a large semi-arid floodplain: Implications for salinity management. *Hydrol. Process.* 19, 3063-3080.
- Laya, H.A., 1981. Relevamiento semidetallado de suelos del valle inferior del río Chubut. In: *Inversiones, C.F.d. (Ed.)*, Chubut, p. 202.
- Letshela, K.P., Atekwana, E.A., Molwalefhe, L., Ramatlapeng, G.J., Masamba, W.R.L., 2023. Stable hydrogen and oxygen isotopes reveal aperiodic non-river evaporative solute enrichment in the solute cycling of rivers in arid watersheds. *Sci. Total. Environ.* 856, 159113.

- Liberoff, A.L., Flaherty, S., Hualde, P., García Asorey, M.I., Fogel, M.L., Pascual, M.A., 2019. Assessing land use and land cover influence on surface water quality using a parametric weighted distance function. *Limnologica*. 74, 28-37.
- Masseroni, D., Ricart, S., De Cartagena, F.R., Monserrat, J., Gonçalves, J.M., De Lima, I., Facchi, A., Sali, G., Gandolfi, C., 2017. Prospects for Improving Gravity-Fed Surface Irrigation Systems in Mediterranean European Contexts. *Water* 9.
- McCallister, S.L., del Giorgio, P.A., 2012. Evidence for the respiration of ancient terrestrial organic C in northern temperate lakes and streams. *Proc. Natl. Acad. Sci.* 109, 16963.
- McGuire, K., McDonnell, J., 2007. Stable isotope tracers in watershed hydrology. In: Michener, R.H., Lajtha, K. (Eds.), *Stable Isotopes in Ecology and Environmental Science*. Blackwell Publishing, pp. 334-374.
- Pascual, M.A., Olivier, T., Brandizi, L., Rimoldi, P., Malnero, H.A., Kaless, G., 2020. Cuenca del Río Chubut. Análisis de Factibilidad para Fondo de Agua. Alianza Latinoamericana de Fondos de Agua, p. 197.
- Pessacq, N., Blázquez, J., Lancelotti, J., Solman, S., 2022. Climate Changes in Coastal Areas of Patagonia: Observed Trends and Future Projections. In: Helbling, E.W., Narvarte, M.A., González, R.A., Villafañe, V.E. (Eds.), *Global Change in Atlantic Coastal Patagonian Ecosystems: A Journey Through Time*. Springer International Publishing, Cham, pp. 13-42.
- Pessacq, N., Flaherty, S., Brandizi, L., Solman, S., Pascual, M., 2015. Getting water right: A case study in water yield modelling based on precipitation data. *Sci. Total. Environ.* 537, 225-234.
- Pessacq, N., Flaherty, S., Solman, S., Pascual, M., 2020. Climate change in northern Patagonia: critical decrease in water resources. *Theoretical and Applied Climatology* 140, 807-822.
- Pulido-Bosch, A., Rigol-Sanchez, J.P., Vallejos, A., Andueza, J.M., Ceron, J.C., Molina-Sanchez, L., Sola, F., 2018. Impacts of agricultural irrigation on groundwater salinity. *Environmental Earth Sciences* 77.
- R Development Core Team, 2020. *R: A Language and Environment for Statistical Computing*. R Foundation for Statistical Computing, Vienna, Austria.
- Sainz-Trápaga, J.M., 2018. Gestión hídrica en el Valle Inferior del Río Chubut. pp. 131. <https://www.repositorio.cenpat-conicet.gov.ar/handle/123456789/123451227>.
- Scanlon, B.R., Jolly, I., Sophocleous, M., Zhang, L., 2007. Global impacts of conversions from natural to agricultural ecosystems on water resources: Quantity versus quality. *Water Resour. Res.* 43.
- Serra, J.J., Malnero, H., De Pablo, F., 2005. Análisis de la capacidad de conducción actual del cauce inferior del Río Chubut. Departamento de Ingeniería Civil Hidráulica, Facultad de Ingeniería, Universidad Nacional de la Patagonia San Juan Bosco, p. 13.
- Stampone, J.E., 2003. *Geología: una visión a partir del cosmos*. Universidad Nacional de la Patagonia San Juan Bosco, Chubut, Argentina.
- Stampone, J.E., 2012. Estudio hidrogeológico. Zona del matadero municipal. Localidad de 28 de Julio. Comisión de Fomento de 28 de Julio, Chubut, Argentina, p. 18.
- Thomas, L.K., Tölle, L., Ziegenhagen, B., Leyer, I., 2012. Are Vegetative Reproduction Capacities the Cause of Widespread Invasion of Eurasian Salicaceae in Patagonian River Landscapes? *PLOS ONE* 7, e50652.
- Torres, A.I., Niencheski, L.F.H., Campodonico, V.A., Pasquini, A.I., Faleschini, M., Depetris, P.J., 2021. Hydrochemical Insight and Groundwater Supply: A Case Study of Patagonia's Chubut River. In: Häder, D.-P., Helbling, E.W., Villafañe, V.E. (Eds.), *Anthropogenic Pollution of Aquatic Ecosystems*. Springer International Publishing, Cham, pp. 205-228.
- Yang, K., Han, G., 2020. Controls over hydrogen and oxygen isotopes of surface water and groundwater in the Mun River catchment, northeast Thailand: implications for the water cycle. *Hydrogeology Journal* 28, 1021-1036.

Author Statement

Ana Laura Liberoff: Project administration, Conceptualization, Methodology, Investigation, Writing - Original Draft, Visualization

María Poca: Formal analysis, Writing - Original Draft,

Journal Pre-proof

Declaration of interests

The authors declare that they have no known competing financial interests or personal relationships that could have appeared to influence the work reported in this paper.

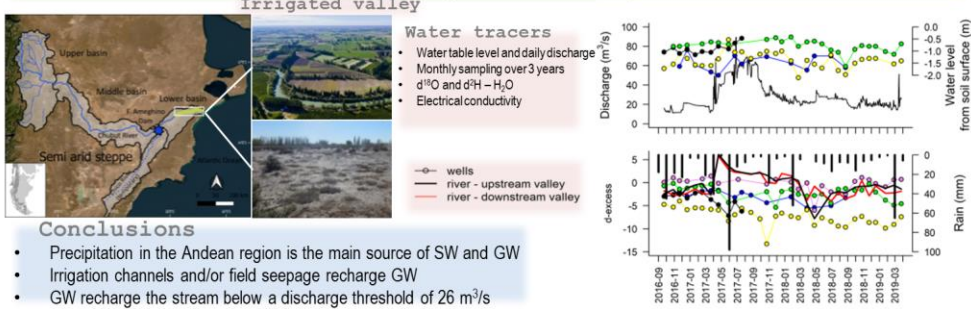
The authors declare the following financial interests/personal relationships which may be considered as potential competing interests:

Ana Laura Liberoff reports financial support, equipment, drugs, or supplies, and travel were provided by International Atomic Energy Agency. Ana Laura Liberoff reports financial support and equipment, drugs, or supplies were provided by Agencia Nacional de Promoción de la Investigación, el Desarrollo Tecnológico y la Innovación. Ana Laura Liberoff reports equipment, drugs, or supplies and travel were provided by Consejo Nacional de Investigaciones Científicas y Técnicas.

Graphical abstract

Objective

Evaluate the effect of surface irrigation on the surface (SW) – groundwater (GW) interactions and implications on river dynamics in a semiarid valley



Conclusions

- Precipitation in the Andean region is the main source of SW and GW
- Irrigation channels and/or field seepage recharge GW
- GW recharge the stream below a discharge threshold of 26 m³/s

Journal Pre-proof

Highlights

- Groundwater levels are high and fluctuate seasonally with irrigation schedule.
- Mobilization of stored salt in the soil and field seepage might be increasing groundwater salinity.
- Plant transpiration and evaporation in the upper and middle basins increase river salinity.
- River salinity in the lower basin is mainly regulated by the reservoir dynamics and closing and opening of irrigation channels.
- Below a daily discharge threshold of 26 m.s^{-1} groundwater recharge the stream affecting river salinity.

Journal Pre-proof